

Fig. 2. The monochromatic flux emitted at 3,000 Mc/s as a function of linear size. Upper limits on size are indicated by arrows. Sources with spectral indices greater than -0.5 are denoted by filled circles, and those with indices less than -0.5 by open circles. The dashed line connects two points plotted for 3C 273.

puted and are shown in Fig. 2. Again the stronger sources have smaller dimensions than the weaker sources. There is a large scatter in size for a given luminosity, which might in part arise from projection effects. For example, if the axes of double sources are randomly oriented and if for a given luminosity all sources have the same component separation d , then two-thirds of the sources would have apparent separations between $0.5d$ and d . Since the scatter is larger than this, there must also be a dispersion in the intrinsic sizes of the sources. This conclusion is supported by the example of 3C 273, in which the separation of components A and B is fifty times that of the small double within B .

Fig. 2 also shows the relationship between the spectra of quasi-stellar sources and their sizes. A spectral index has been derived from the fluxes at 1,400 and 2,695 Mc/s. Those sources with spectral indices greater than -0.5 are indicated by filled circles, and those with indices less than -0.5 by open circles. All the large sources have steep spectra. Among the smaller sources there is a dispersion of indices; it is clear, however, that if a source has a flat spectrum, it will be small.

I thank K. Kellermann and I. Pauliny-Toth, who provided the 2,695 Mc/s flux densities, and S. von Hoerner for his helpful comments. The models for three of these sources were provided by B. G. Clark.

D. E. HOGG

National Radio Astronomy Observatory,
Green Bank, West Virginia.

Received October 31, 1966.

¹ Clark, B. G., and Hogg, D. E., *Astrophys. J.*, **145**, 21 (1966).

² Wyndham, J. D., *Astrophys. J.*, **144**, 459 (1966).

³ Burbidge, G. R., Burbidge, E. M., Hoyle, F., and Lynds, C. R., *Nature*, **210**, 774 (1966).

⁴ Schmidt, M., *I.A.U. Symposium on Instability Phenomena in Galaxies* (Bjurakan, May, 1966).

⁵ Adgie, R. L., Gent, M., Slee, O. B., Frost, A. D., Palmer, H. P., and Rowson, B., *Nature*, **205**, 275 (1965).

⁶ Kellermann, K. I., and Pauliny-Toth, I., *Nature*, **212**, 781 (1966).

Role of Acceleration in Relativistically Expanding Objects and its Significance for the Intensity Variations in Quasi-stellar Sources

REES¹ has discussed the appearance of relativistically expanding objects as seen by distant observers, with a view to explaining the variation of flux from radio sources. There he considers a spherical shell expanding with a uniform radial velocity $v \sim c$. The apparent radius of the source at time t_0 , measured from the moment when the

expansion is seen to begin, is γvt_0 , where $\gamma = (1 - v^2/c^2)^{-1/2}$. The Doppler blue-shift, measured as the ratio of frequency observed to frequency emitted, varies from γ on the limb to $\gamma[1 + v/c]$ in the centre. The effect of special relativity in Rees's model is to cut down the apparent time scales, in the cases where γv is greater than c . The actual variation of flux is obtained from an astrophysical model. Such a model might work for radio variations, but not for optical variations of quasi-stellar sources.

The purpose of this communication is to point out the effect of acceleration in a relativistically expanding object. As the following calculations will show, the front part of the object has a rapidly rising blue-shift which could cause a sudden rise in the observed intensity of the source. Since this is a pure Doppler effect it could work in optical as well as radio frequency range.

Consider a sphere with centre S , expanding radially outwards. Let $r(t)$ denote the radius of the sphere at time t after the expansion started, t being measured in the rest frame of S . The effects of the expansion of the universe (if any) will be neglected in the present calculations. The locus of points on the object from which radiation reaches a distant observer O at rest relative to S at the same time is a surface of revolution about SO . The section of this surface through SO is a curve given by

$$t - \frac{r(t)}{c} \cos \theta = t_0 \tag{1}$$

where t_0 is the time elapsed since the expansion was seen to begin and θ is the angle measured from SO of the velocity of ejection from S . At any given t_0 , equation 1 determines r as a function of θ for any specified $r(t)$. A simple calculation shows that the apparent radius of the limb, that is, the maximum value of $r \sin \theta$, is given by

$$r_0 = r(t)[\gamma(t)]^{-1} \tag{2}$$

where

$$\gamma(t) = (1 - v^2/c^2)^{-1/2}, \quad v = \frac{dr}{dt} \tag{3}$$

and t in $r(t)$ is determined from

$$t - \frac{r(t)v(t)}{c^2} = t_0 \tag{4}$$

The corresponding value of θ is given by

$$\cos \theta_0 = v(t)/c \tag{5}$$

If the object is opaque, only those parts the velocity of which makes an angle less than θ_0 with SO will be visible. The apparent rate of increase of the limb radius is

$$\frac{dr_0}{dt_0} = \gamma(t)v(t) \tag{6}$$

In the case considered by Rees, $v(t)$ is constant and these results are much simplified.

So far, the form of the function $r(t)$ has not been specified. In the case of uniform acceleration from rest $r(t)$ is given by

$$r(t) = \frac{c^2}{f} [(1 + f^2 t^2/c^2)^{1/2} - 1] \tag{7}$$

Here f is the acceleration defined in a relativistically invariant way.

The substitution of this $r(t)$ in equations 2-4 gives

$$v(t) = \frac{ft}{(1 + f^2 t^2/c^2)^{1/2}} = ft_0 \tag{8}$$

$$r_0 = \frac{c^2}{f} [1 - (1 - f^2 t_0^2/c^2)^{1/2}] \tag{9}$$

Thus uniform acceleration cannot be observed from O , for t_0 is greater than c/f by the rays coming from the limb. The blue-shift varies from γ at the limb to $\gamma^2(1 + v/c)$ in the centre. The blue-shift varies more rapidly from the limb to the centre than in the case discussed by Rees because the centre is observed at a later stage of the expansion than the limb.

As t_0 approaches c/f (that is, as the velocities become highly relativistic) the blue-shift rises very rapidly, for from equation 8 we get

$$\frac{d\gamma}{dt_0} = \frac{f^2 t_0}{c^2} [1 - f^2 t_0^2 / c^2]^{-3/2} \quad (10)$$

Consider now an object emitting jets of particles which have been uniformly and simultaneously accelerated from rest. If the acceleration continues up to relativistic velocities, such a jet would exhibit a rapidly rising blue-shift to an observer facing it. The effect of this blue-shift is to increase rapidly any flux of radiation emitted by the particles, whether in the optical or in the radio range. The effect is one of acceleration—not of velocity—and will discontinue once the acceleration has ceased.

I thank Professor F. Hoyle for useful discussions.

J. V. NARLIKAR

King's College,
Cambridge.

Received October 27, 1966.

¹ Rees, M. J., *Nature*, 211, 468 (1966).

PLANETARY SCIENCE

Spectral Types of Decametric Radiation from Jupiter

EXPERIMENTS relating to the spectral fine structure of decametric radiation from Jupiter have been described^{1,2}. During the opposition of the planet in 1965 the high-resolution spectral experiment was repeated. The main equipment was the 14-channel spectrograph² with channel-to-channel spacing of 50 kc/s and a frequency centred on 19.1 Mc/s. Some modifications were made to the antenna and display system so that the recording time constant was approximately 40 msec. I operated the spectrograph for 3–4 h each night from October 1 to December 31, 1965, at the Radio Astronomy Station of the University of Helsinki.

The new results support the earlier ones. There are indications of three types of dynamic spectra of high resolution and there are also bursts which have bandwidths of the order of 50 kc/s.

The most common type of spectrum is a structure with practically no details. It can appear as a smooth, vertical

or slightly tilted bar in spectra where the horizontal scale represents time. Typical bandwidths are 0.5 Mc/s or more (the working range of the present spectrograph is 650 kc/s) while the duration of the spectra are a few seconds; bursts lasting up to 1 min are less frequent.

The second spectral type has more details. It is composed of bursts which often have bandwidths of the order of 50 kc/s. The duration of individual bursts is of the order of 1 sec. Such a spectrum has the appearance of an irregular group of flecks and patches.

The third type is very complex. It is composed of pulses which may have bandwidths down to 50 kc/s, while their duration often goes down to the time resolution limit of the equipment. The pulses can recur at intervals ranging from a fraction of a second to several seconds.

In this report these three spectral types are classified as *A*, *B* and *S*, respectively. This is slightly different from my earlier classification². The type *A* emission occurs most often when the principal source, or source *A*, is in the central meridian; similarly the type *B* emission seems to favour the situation of source *B* in the central meridian. The source designation is that of Carr *et al.*³. The *S* type is probably the same as the phenomenon called *S* pulses by Gallet⁴ on the basis of single-frequency observations and the same as the "spitting" noise (because of its aural characteristics) of Carr *et al.*⁵, also on single-frequency observations. Typical spectra of types *A* and *S* are reproduced in Fig. 1.

In Fig. 2 the number of events is shown as a function of System III central meridian longitude. Activity, irrespective of its duration, is counted only once for each 5° interval in the central meridian. The *S* profile seems to have two sources separated by approximately 180°.

In Fig. 3 the number of events is plotted as a function of Io's longitude on System III. In this plot the *A* profile is broader, the *B* profile narrower, and the two sources of the *S* profile merge together, if compared with Fig. 2. If the plot is made in a third way as a function of Io's longitude measured from its geocentric conjunction, as introduced by Bigg⁶, the *S* profile shows two sources.

One of the possible reasons leading to the similarities of *B* and *S* profiles could be the insufficient resolution in time. A very dense *S* type emission could remain unresolved and, if confined to a narrow band, may appear as type *B*.

This experiment strongly suggests that there may be considerable variations in the bandwidth properties of Jovian decametric bursts. It is therefore doubtful whether

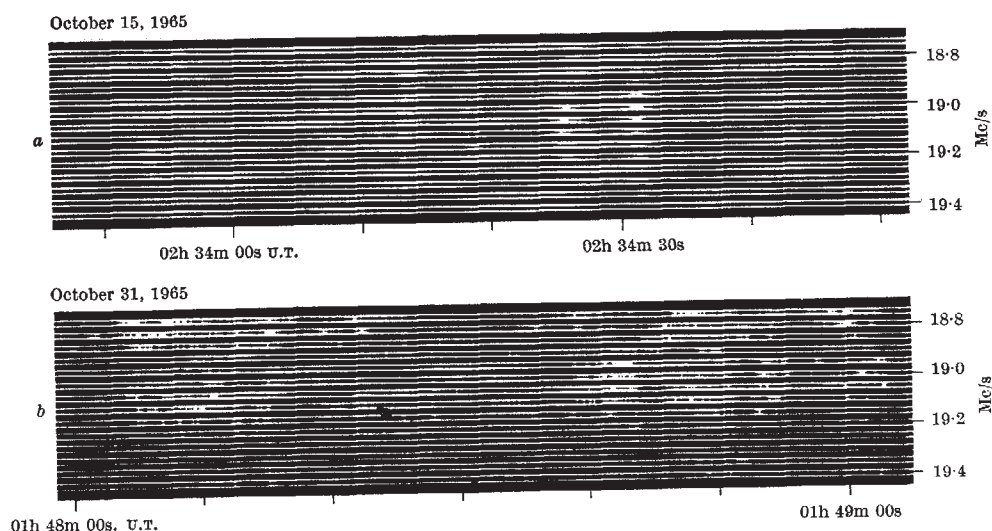


Fig. 1. Decametric Jovian radio bursts recorded with a high-resolution 14-channel radio spectrograph. The channel output indicators are area-modulated and photographed on a continuously moving film. Each track closes with an increase in the signal level in the corresponding channel. An example of a type *A* burst is shown in (a) and a type *S* burst in (b).